Cement and Concrete Research 40 (2010) 1298–1305

Contents lists available at ScienceDirect

Cement and Concrete Research

journal homepage: http://ees.elsevier.com/CEMCON/default.asp

# Geochemical modeling of leaching of Ca, Mg, Al, and Pb from cementitious waste forms

E. Martens [a,*], D. Jacques [a], T. Van Gerven [b], L. Wang [a], D. Mallants [a]

[a] Belgian Nuclear Research Centre (SCK•CEN), Institute for Environment, Health, and Safety, Boeretang 200, B-2400 Mol, Belgium
[b] Katholieke Universiteit Leuven, Faculty of Engineering, Dept. of Chemical Engineering, de Croylaan 46, B-3001 Leuven, Belgium

ARTICLE INFO

*Article history:*
Received 19 May 2009
Accepted 8 January 2010

*Keywords:*
Lead (D)
Portland cement (D)
Modeling (E)
Waste management (E)
Leaching

ABSTRACT

Results from extraction tests on cement–waste samples were simulated with a thermodynamic equilibrium model using a consistent database, to which lead data were added. Subsequent diffusion tests were modeled by means of a 3D diffusive transport model combined with the geochemical model derived from the extraction tests.

Modeling results of the leached major element concentrations for both uncarbonated and (partially) carbonated samples agreed well with the extraction test using the set of pure minerals and solid solutions present in the database. The observed decrease in Ca leaching with increasing carbonation level was qualitatively predicted. Simulations also revealed that Pb leaching is not controlled by dissolution/precipitation only. The addition of the calcite–cerrusite solid solution and adsorption reactions on amorphous Fe- and Al-oxides improved the predictions and are considered to control the Pb leaching during the extractions tests. The dynamic diffusive leaching tests were appropriately modeled for Na, K, Ca and Pb.



## 1. Introduction

Solidification/stabilization (S/S) is a technique for immobilizing hazardous wastes in binding materials, mostly cement-based, to delay the release of toxic components to the environment. Chemical waste is often S/S treated and is then landfilled or recycled into new building materials. The technique is also applied for large amounts of low-level radioactive wastes which are conditioned with cementitious materials to provide a safe disposal leading to only negligible radiological impact on humans and the environment. In both cases, the waste streams that undergo a S/S treatment contain a number of chemically toxic elements, such as Cd, Ni, Pb, Sb, Zn, etc. Sooner or later, the S/S waste will be contacted with water and leaching might cause a (partial) remobilization of toxic elements. It is thus extremely important to understand the leaching behaviour of the different elements. Depending on process parameters such as pH, different processes may occur, e.g. surface complexation, dissolution/precipitation, sorption and incorporation to a mineral phase. Leaching tests and subsequent geochemical modeling are typically used to investigate the leaching behaviour of the pollutants. Leaching tests allow to determine the parameters that control the release of the elements of concern and the amounts that are released. The short-term behaviour is examined by extraction tests, while diffusion tests provide information for longer timescales. Geochemical modeling then helps to interpret the leaching tests, i.e. it is an important tool to gain insight into the complex leaching mechanisms that are responsible for the observed release patterns. As extraction tests are less time-consuming than diffusion tests, they are most commonly applied. As such, many studies are available on the modeling of extraction tests for different elements considering leaching from uncarbonated samples [1,2] as well as from carbonated samples [3–7]. The composition of the samples varies from pure ashes or cement to mixtures of these two. Far less work has been performed on modeling diffusion tests. One dimensional reactive transport simulations were performed by a number of authors [8–10], but to our knowledge only De Windt et al. [11] developed a three dimensional model.

In this study, release data for the major elements Na, K, Ca, Mg and Al and one contaminant (Pb) leached from uncarbonated and carbonated ordinary Portland cement (OPC)—dried bottom ash from municipal solid waste incinerator (MSWI) samples during extraction and diffusion tests were modeled using the geochemical transport code PHREEQC-2.15 [12]. Martens et al. [13] already modeled the data from the extraction tests by means of a stepwise selection of minerals controlling the solubility of the major elements Ca, Mg and Al. A good agreement between experiments and model simulations was obtained. However, a thermodynamic database including data from different sources was applied, so the consistency of the database could not be guaranteed. Recently, a consistent thermodynamic database for cement systems called CEMDATA07.1 was published [14]. In the title study, the data from the CEMDATA07.1 database is applied. The

* Corresponding author.
*E-mail address:* evelien.martens@csiro.au (E. Martens).

0008-8846/$ – see front matter © 2010 Elsevier Ltd. All rights reserved.
doi:10.1016/j.cemconres.2010.01.007

objectives were thus (i) to ascertain if the set of pure mineralogical phases and solid solutions present in the consistent CEMDATA07.1 database extended with thermodynamic data for Pb speciation is sufficient to describe the results of the extraction test regarding leached concentrations of Ca, Mg, Al and Pb for both the uncarbonated and carbonated samples, and (ii) to apply the model verified with the static extraction tests for simulating the diffusion tests performed on uncarbonated concrete/waste samples.

## 2. Experimental data

Mortars with a water-to-cement ratio of 0.5 were prepared by mixing 548 kg/m$^3$ of OPC (CEM I 42.5 R HES, Holcim), 1096 kg/m$^3$ dried MSWI bottom ash (the 0–2 mm fraction of a MSWI bottom ash that underwent a wet-sieving treatment as described in [15]) and 281 kg/m³ distilled water. The mixtures were poured in moulds of 150×150×150 mm and vibrated. After a 24 hour setting time, the samples were demoulded and cured for 28 days in a humid room (20 °C, >95% relative humidity (RH) and 0.035% $CO_2$). The uncarbonated sample was obtained by removing a layer of about 1.5 cm of material from the edges of the cubes. Sample cubes of 40×40×40 mm were prepared using a dry cutting technique. Uncarbonated samples (indicated as "B0" from here on) were dried in a vacuum oven at 40 °C and stored at room temperature in a $CO_2$ free bag filled with nitrogen gas. The carbonated samples were prepared by conditioning fresh non-crushed samples for 14, 30 and 60 days in a closed chamber at 37 °C, >90% RH and 20% $CO_2$, indicated respectively as "B14", "B30", and "B60" further in the paper. After 60 days, the samples were completely carbonated. Samples B14 and B30 are thus partially carbonated whereas B60 is nearly completely carbonated.

A series of single extraction tests was conducted on each set of cubes using 10 g of particle-size reduced material (more than 95 wt.%< 125 μm) in 100 ml distilled water acidified with different volumes of concentrated $HNO_3$ (analogous to the EN12457 test [16]) resulting in a pH range from 1 to 12. The pH and composition of the leachate were analysed after 24 h of contact time. For selected samples, extraction tests longer than 1 day (up to 2 weeks) were performed but no significant changes were observed for the elements reported in this paper. Detailed experimental procedures and discussion of the experimental data are given in [17].

Diffusion tests were conducted on three uncarbonated samples. A semi-dynamic monolith leaching procedure was applied, by modifying the Dutch diffusion test NEN 7345 [18] by prolonging exposure to a cumulative 225 leaching days. Each monolith was immersed in 320 ml of distilled water (acidified to pH 4 with concentrated $HNO_3$) that was collected and renewed with fresh leachant 17 times after cumulative leaching times of 6, 24, 54, and 96 h and 9, 16, 25, 36, 49, 64, 81, 100, 121, 144, 169, 196 and 225 days. After each renewal an aliquot of the leachate was filtered through a 0.45 μm membrane, 50 ml of the filtered sample was acidified with concentrated nitric acid to pH<1 (to avoid precipitation of metals during storage) and conserved for measurement. More details on the experimental procedure and discussion of the experimental data are given also in [17].

The amounts of hydrous ferric oxides (HFO) and amorphous aluminium minerals (AAM) were determined on B0 and B60 samples, to estimate the adsorption capacity for Pb by surface complexation. To determine the HFO content in MSWI bottom ash, the method of Ferdelman [19] by which HFO is selectively extracted by ascorbate, was used. HFO contents for B0 and B60 samples are 1.31 g/l (one measurement) and 0.62 g/l (average of two repetitions), respectively. AAM was measured by oxalate extraction in the dark [20], giving values of 3.07 g/l and 3.25 g/l for the B0 and B60 sample, respectively (each an average of three repetitions). Additional details on the extraction procedures are given in [21].

## 3. Thermodynamic data and model features

### 3.1. Computer code and thermodynamic data

Data from the recently published consistent thermodynamic database for cement systems CEMDATA07.1 is applied to model the extraction and diffusion tests with the geochemical code PHREEQC-2.15. This database includes several cement hydrates for ordinary Portland cement systems, such as the calcium silicium hydrates (C–S–H phases) which are described by a solid solution model, AFm phases (as monocarboaluminate, strätlingite), AFt phase (ettringite and tricarboaluminate), hydrogarnet, and hydrotalcite. The implementation of the CEMDATA07.1 data (originally written for GEMS [22] format) in PHREEQC was verified by [23] and the complete dataset is used in the title study. Only one modification to the CEMDATA07.1 was made: the solid solution tobermorite-I — $SiO_2$(am) was replaced by a pure $SiO_2$(am) phase as this solid solution may not exist or is not ideal [23]. All the minerals and aqueous species present in the CEMDATA07.1 database that consists of elements considered in this study (cf. Section 3.2) can be formed in the simulations. The minerals from the CEMDATA07.1 database are listed in Appendix A.

Thermodynamic data for lead are added as these were not yet included in CEMDATA07.1. Lead aqueous species (hydroxyl, chloride, carbonate and sulfate species) as well as five lead minerals were included, i.e. anglesite ($PbSO_4$), lead sulfide (PbS), lead hydroxide ($Pb(OH)_2$), hydrocerrusite ($Pb_3(CO_3)_2(OH)_2$) and cerrusite ($PbCO_3$, present as a pure mineral or as an end-member in the ideal (Pb,Ca)$CO_3$ solid solution). The formation of a calcite–cerrusite solid solution is suggested by different authors [24–26]. Thermodynamic data for the lead minerals are shown in Table 1 and were based on [27]. Apart from solubility and solid solution mechanisms, Pb leaching may also be affected by sorption. Pb sorbs on HFO [28–31] and AAM [29,32]. These two sorbing minerals were thus included in the model. The sorption sites on HFO are divided into low-capacity/high-affinity sites (HFO_s) and high-capacity/low-affinity sites (HFO_w) with sorption densities of $5 \cdot 10^{-3}$ mol/mol Fe for HFO_s and 0.2 mol/mol Fe for HFO_w [28]. The number of reactive sites is obtained from the measured amount of HFO and the molecular weight of 89 g HFO/mol Fe [28]. Values for total sorption sites on HFO and AAM are given in Table 2. Because of lack of appropriate data, the reactive sites on AAM were calculated using the same specific surface area and concentration of binding sites as for HFO, using the latter as a surrogate for the former, although AAM have a lower surface area than HFO [33]. Thermodynamic constants for the surface complexation reactions (Table 3) are from [28], but the log($K$) for surface complexation on the weak sites was increased from 0.3 to 1.7 as suggested by [29], using a general trend of 3 log units difference between complexation constants for high- and low-affinity sites. Finally, many authors indicate ettringite and C–S–H as prime candidates for heavy metal binding (e.g., [34–41]). Moulin et al. [36] carried out sorption isotherms of Pb on non-hydrated as well as hydrated calcium silicate, for Pb trace concentrations (below the solubility of PbO). This study showed that Pb has a high affinity for calcium silicate in both hydration states. A $^{29}$Si nuclear magnetic resonance study in the same

**Table 1**
Thermodynamic data for lead minerals.

| Mineral | Reaction | Log $K$ | Reference |
|---|---|---|---|
| Cerrusite (s) | $PbCO_3 = Pb^{2+} + CO_3^{2-}$ | −13.2 | [27] |
| Hydrocerussite (s) | $Pb_3(CO_3)_2(OH)_2 + 2\ H^+ = 3\ Pb^{2+} + 2\ H_2O + 2\ CO_3^{2-}$ | −17.6 | [27] |
| PbS (s) | $PbS + H^+ = Pb^{2+} + HS^-$ | -12.2 | [27] |
| Anglesite (s) | $PbSO_4 = Pb^{2+} + SO_4^{2-}$ | −7.8 | [27] |
| $Pb(OH)_2$ (s) | $Pb(OH)_2 + 2\ H^+ = Pb^{2+} + 2H_2O$ | 9 | Adjusted from [27] |

**Table 2**
Total number of sorption sites on HFO and AAM.

| Sample | HFO_w (mol/l) | HFO_s (mol/l) | AAM_w (mol/l) | AAM_s (mol/l) |
|---|---|---|---|---|
| B0 | $2.95\times10^{-3}$ | $7.37\times10^{-5}$ | $6.89\times10^{-3}$ | $1.72\times10^{-4}$ |
| B60 | $1.38\times10^{-3}$ | $3.46\times10^{-5}$ | $7.31\times10^{-3}$ | $1.83\times10^{-4}$ |

**Table 4**
Thermodynamic data for the alkali oxides.

| Reaction | Log *K* | Reference |
|---|---|---|
| $Na_2O + 2\,H^+ = H_2O + 2Na^+$ | 24.94 | [44] |
| $K_2O + 2\,H^+ = H_2O + 2K^+$ | 25.71 | [44] |

publication revealed that Pb is fixed to C–S–H through a Pb–O–Si bond. The latter was confirmed and the structure of the bond was further revealed in an X-ray absorption spectroscopy study performed by Rose et al. [37]. However, for ettringite as well as for C–S–H, the binding mechanisms are still not determined unequivocally and/or thermodynamic data are lacking or incomplete. Binding to ettringite and C–S–H were therefore not included in the geochemical model.

As in the CEMDATA07.1 database, the extended Debye–Hückel equation in the Truesdell–Jones form is used to compute the activity coefficients of aqueous species.

### 3.2. Model description of the initial system

#### 3.2.1. Extraction test

The initial condition was defined by the total concentrations of the elements (Si, Ca, Al, Mg, S(6), Na, K, Pb, Cl and C) measured in the solid samples at the start of the extraction test, except for Si and C. Preliminary simulations indicated that leachate Ca concentrations are underpredicted by several orders of magnitude when the total Si concentration is used. The maximum measured leachate Si concentration (for uncarbonated samples, data from [42]) was only 106 mmol/l (liquid-to-solid ratio = 10, pH = 2) compared to a total measured concentration of 917 mmol/l. Simulation results for Ca became more acceptable when this maximum measured leachate Si concentration was used as input concentration. For the carbonated series, leachate Ca concentrations were underpredicted when the total C concentration is used (results not shown), which was also observed in other studies [3,6,35] indicating either inappropriate thermodynamic data or slow reaction kinetics. Alternatively, a part of the carbonate is not available for reaction with Ca because it is possibly incorporated in stable cement phases [5,43]. The active carbonate concentration is therefore deduced from the difference between the free portlandite in uncarbonated and carbonated samples assuming that free portlandite is transformed into calcite. Reported ratios between total measured carbonate concentrations and calculated active ones ranged between 2.5 [5] and 3 [43]. A value of 2.75 is adapted in this study.

#### 3.2.2. Diffusion test

The initial condition was defined by the total concentrations of the elements measured in the solid samples at the start of the diffusion test. Total concentration was then divided between solid and liquid phases based on the chemical equilibrium of the cement phases.

In the extraction test, pH was regulated by addition of $HNO_3$. In the PHREEQC file, pH was fixed to the desired values (i.e. pH was varied between 1 and 13 with steps of 0.5). In the diffusion test, there is no pH-control. As such, leaching of Na and K ions may have a significant influence on the pH level (as these ions are charge balanced by hydroxide ions) and thus need to be predicted accurately. As beside syngenite no Na- and K-containing minerals are included in the CEMDATA07.1 database, the maximum leachable concentrations of Na and K (determined by performing a NEN7341 test, [43]) were used as input value and the approach of Wang [44] was used: the log(*K*) values of alkali oxides (Table 4) were chosen so that dissolution of

**Table 3**
Thermodynamic constants for the surface complexation reactions.

| Site | Reaction | Log *K* | Reference |
|---|---|---|---|
| Weak site | $Hfo\_wOH + Pb^{2+} = Hfo\_wOPb^+ + H^+$ | 1.7 | [29] |
| | $Hfo\_wOH + Ca^{2+} = Hfo\_wOCa^+ + H^+$ | −5.85 | [28] |
| | $Hfo\_wOH + Mg^{2+} = Hfo\_wOMg^+ + H^+$ | −4.6 | [28] |
| | $Hfo\_wOH + SO_4^{2-} + H^+ = Hfo\_wSO_4^- + H_2O$ | 7.78 | [28] |
| | $Hfo\_wOH + SO_4^{2-} = Hfo\_wOHSO_4^{2-}$ | 0.79 | [28] |
| | $Hfo\_wOH + CO_3^{2-} + H^+ = Hfo\_wCO_3^- + H_2O$ | 12.56 | [50] |
| | $Hfo\_wOH + CO_3^{2-} + 2\,H^+ = Hfo\_wHCO_3 + H_2O$ | 20.62 | [50] |
| Strong site | $Hfo\_sOH + Pb^{2+} = Hfo\_sOPb^+ + H^+$ | 4.65 | [28] |
| | $Hfo\_sOH + Ca^{2+} = Hfo\_sOHCa^{2+}$ | 4.97 | [28] |

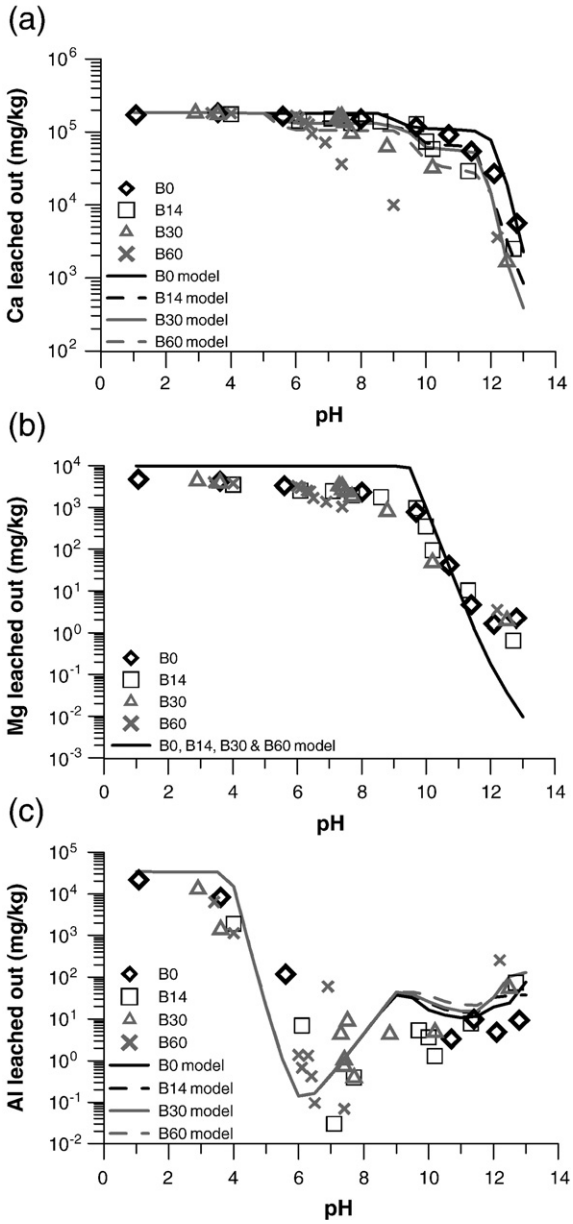


**Fig. 1.** Comparison between calculated and measured leachate concentrations of (a) Ca, (b) Mg, and (c) Al for uncarbonated (B0) and three levels of carbonated (B14, B30, B60) OPC-MSWI bottom ash samples.

$Na_2O$ and $K_2O$ in pore water will result in dissolved Na and K concentrations of 0.14 and 0.37 m respectively. These are the experimental observed average Na and K concentrations in an OPC pore fluid [45].

As some dissolution of atmospheric carbon dioxide followed by precipitation of carbonates was observed in the experiments, this was also included in the model, i.e. the water was equilibrated with atmospheric carbon dioxide and precipitation of calcite and cerrusite was allowed.

## 4. Results and discussion

### 4.1. Extraction tests

#### 4.1.1. Leaching of major elements

Fig. 1 compares the experimental and calculated leachate concentrations for the major elements Ca, Mg and Al. Overall, predictions describe the observed trends relatively well. The model is able to predict the leached concentrations within one or two orders of magnitude, for fresh, partially and fully carbonated cementitious waste samples. The model also qualitatively reproduces the decreased Ca leaching with increasing degree of carbonation, although between pH 6 and 12, the quantitative match between model and experiment is less satisfying for the more carbonated samples (B30 and especially B60). Further, the simulations show that a large set of minerals controls the Ca leaching (Fig. 2), the most important minerals being portlandite (only for B0), the jennite-like and tobermorite2-like solid solution end-members, strätlingite and calcite (not for B0). The decalcification process is illustrated in the changing amounts of the C–S–H solid solution end-members, i.e. the more carbonated the sample, the more tobermorite2-like end-member (Ca/Si ratio = 0.83) and the less jennite-like end-member (Ca/Si ratio = 1.67) are predicted to form. Also monosulfoaluminate, hydrogarnet-OH and $C_4AH_{13}$ dissolve to supply additional Ca-ions for the formation of carbonates (calcite and monocarboaluminate).

The Al data show a large degree of scatter at lowest solubility, probably due to concentrations close to the detection limit. There is no real trend visible in the experimental data between the different carbonation levels. This observation is consistent with the modeled behaviour, in which the Al-controlling phases (i.e. strätlingite, hydrogarnet-OH, $C_4AH_{13}$, monosulfoaluminate, monocarboaluminate, tricarboaluminate, ettringite, and amorphous $Al(OH)_3$) are more or less independent of carbonation level, whereas the strong pH-dependency of the solubility of amorphous $Al(OH)_3$ is considered as the most important factor controlling Al leaching.

For Mg, the same can be said as for Al, i.e. there is no real trend visible in the experimental data between the different carbonation levels, which is consistent with the modeled behaviour. Mg leaching is very well predicted by the solubility of brucite, except for the highest pH values (pH ≥ 12).

#### 4.1.2. Leaching of lead

In order to assess the influence of the different processes described in Section 3.1 on Pb leaching, one process was added at a time and three simulations were thus run: (i) in simulation 1 only dissolution/precipitation reactions of the lead minerals were included in the model, (ii) in simulation 2, Pb surface complexation on HFO and AAM was added, and (iii) in simulation 3, calcite and cerrusite were defined as end-members of the ideal $(Ca,Pb)CO_3$ solid solution.

Fig. 3 shows predictions of Pb leaching for the three simulations. In each case, the model predicts the amphoteric Pb leaching profile, but the first simulation does not give good predictions for pH values lower than 8, both for carbonated and uncarbonated samples. Compared to the first simulation, adding Pb surface complexation (simulation 2)

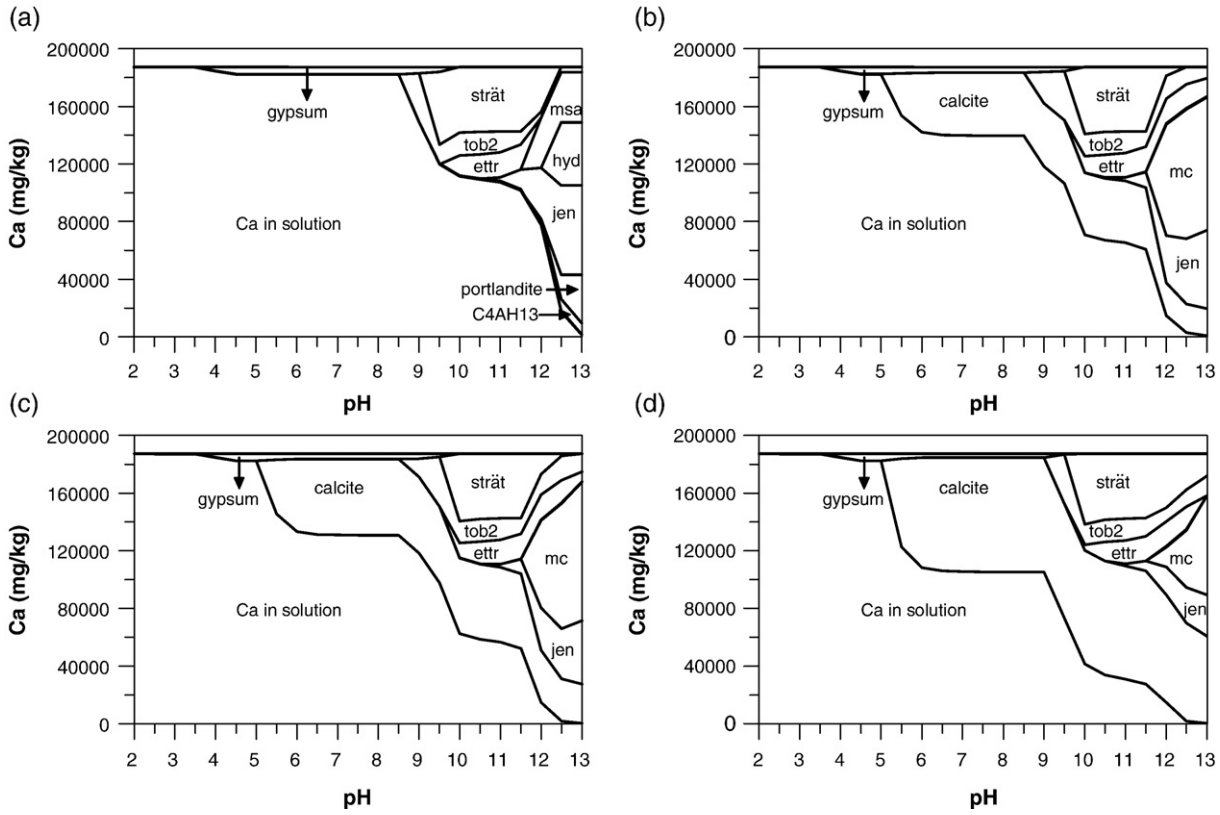


**Fig. 2.** Modeled calcium distribution in solution or mineral phases for sample B0 (a), B14 (b), B30 (c) and B60 (d). Abbreviations used are as follows: ettr = ettringite, hyd = hydrogarnet-OH, jen = jennite-like solid solution end-member, msa = monosulfoaluminate, mc = monocarboaluminate, strät = strätlingite and tob2 = tobermorite2-like solid solution end-member.

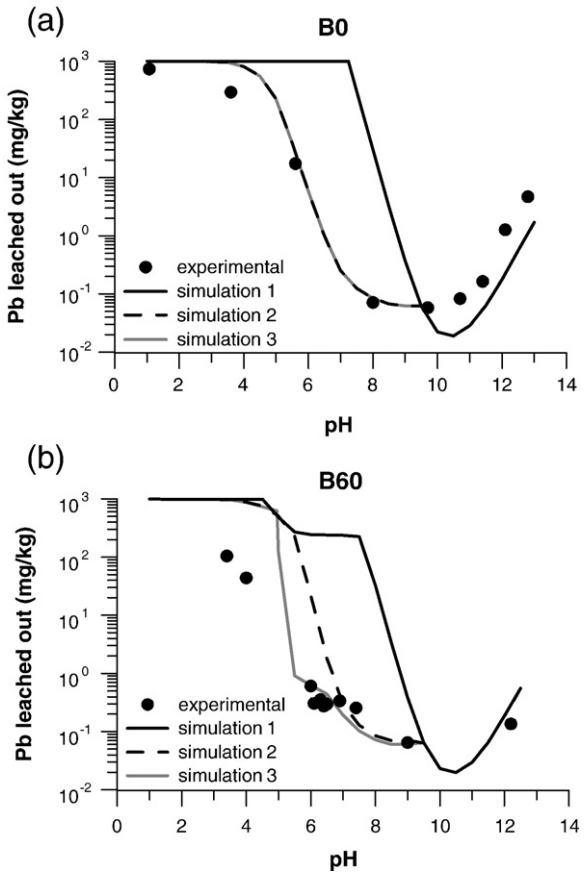


**Fig. 3.** Comparison of the experimental and modeled Pb leaching curves for (a) the uncarbonated sample B0 and (b) the carbonated sample B60. Note that the curves from simulations 2 and 3 coincide for the uncarbonated sample and the curves from simulations 1, 2 and 3 coincide at a pH above approximately 10 for both samples.

improves significantly the prediction of Pb leaching in the lower pH range. Note however that the number of reactive sites on AAM might be overestimated because the same number of reactive sites per gram material as for HFO was assumed. However, the total sorbent concentration measured in this study (4.38 g/l) corresponds well with the value obtained by Meima and Comans [46] (5.06 g/l) for a fresh MSWI bottom ash sample. On the other hand, not all reactive sites are included in the model. For example, crystalline Fe-oxides (formed from HFO) have a smaller, but still significant specific surface area (e.g., 600 and 100 $m^2/g$ for HFO and crystalline iron oxides, respectively, [2]). As the ascorbate extraction technique only measured HFO content, total adsorption capacity might be underestimated. An alternative is using dithionite extraction [47] measuring amorphous and crystalline iron (hydr)oxides. Experimental data indicate that carbonation (sample B60 in Fig. 3) leads to lower Pb leaching between pH 3 and 6, a behaviour which is not predicted by model 2. Results from simulation 2 do not reflect the effect of carbonation (i.e. almost identical simulation results were obtained for the carbonated and uncarbonated sample) because only a very limited amount of Pb-containing carbonates (cerrusite, hydrocerrusite) are predicted to precipitate. When the ideal binary $(Ca,Pb)CO_3$ solid solution is included (simulation 3), the Pb leaching in the carbonated sample is better predicted due to a much higher cerrusite precipitation in the $(Ca,Pb)CO_3$ solid solution.

In conclusion, it can be said that a model that combines a variety of immobilization mechanisms provides a better match between model and experiment, indicating that Pb leaching across a wide pH range is controlled by dissolution, precipitation, sorption and solid solution formation.

### 4.2. Diffusion tests

The geochemical model discussed previously was extended with a diffusive transport part to describe the diffusion test on the uncarbonated sample. By applying the rules of symmetry, 1/8 of the cement cube was divided into smaller cubes, with sides of 2.5 mm each. The model domain was composed of $8\times8\times8=512$ cells of uniform size. The effective diffusion coefficient, $D_e$, which combines the effect of pore-water diffusion and effective porosity ($D_e=D_p\times\eta_e$) is the only unknown transport parameter and was obtained by fitting the cumulative release profile of sodium (Fig. 4a). The resulting best-fit value for $D_e$ is 7 ($\pm0.35$)$\times10^{-12}$ $m^2/s$. This value is larger than, but still of the same order of magnitude as the best-fit value obtained by De Windt and Badreddine [11], i.e. $D_e=3\times10^{-12}$ $m^2/s$ (also for Na). Similar values have also been reported by Tiruta-Barna et al. [48] for Na, K, Cl and Ca ($5–20\times10^{-12}$ $m^2/s$) and by MacCarter [49] for Cl ($0.14–2.42\times10^{-12}$ $m^2/s$) for the same type of materials. The diffusion coefficient of Na is then assigned to all the other elements. The cumulative and non-cumulative release of K, Ca, Mg, Al and Pb are shown in Fig. 4(b–f). The cumulative release profiles emphasize the initial release and are less sensitive to release at longer timescales, whereas the non-cumulative data show the absolute released concentration at each renewal.

For K, Ca and Pb, model predictions are in good agreement with the data. The cumulative release profiles of Ca and Pb have a particular shape, characterized by an initial fast release, which after the eighth water renewal cycle flattens off. Van Gerven et al. [17] explained this by the dissolution of atmospheric carbon dioxide into the water, followed by the precipitation of calcite and cerrusite. This hypothesis is now confirmed by the model simulations: a simulation not allowing dissolution of atmospheric carbon dioxide into the water led to overprediction of the Ca and Pb release (results not shown) while allowing dissolution of atmospheric carbon dioxide followed by precipitation of carbonates provided good results (Fig. 4c and f). The dissolution of atmospheric carbon dioxide into the water is also visible in the pH diagram (Fig. 5): the experimental as well as measured pH of the leachate water shows a drop from the initial value of 12 to 8.5 after 50 days. The non-cumulative profiles of K and Ca are also in very good agreement. For Pb, the initial release is well predicted but the release at later times is somewhat underestimated. It is possible that a little too much cerrusite precipitates in the model. However it should be noted that the *y*-axis is logarithmic, so in fact in both cases the Pb release at longer timescales is almost equal to zero, i.e. 0.02 $mg/m^2$ in the experiment and 0.0002 $mg/m^2$ in the model. Compared to the initial release (for $t<50$ days) of 0.5–1 $mg/m^2$ (in experiment and model) this amount is negligible.

The 3D diffusion model underpredicts the release of Mg. The initial release ($t<5$ days) is underestimated by 3 orders of magnitude while afterwards the predictions are systematically 2 orders of magnitude too low. As mentioned before, the simulation of the pH of the outer solution is satisfying. The pH of the samples themselves cannot be verified as no measurements were performed. However the simulated pH at the outer cells of the sample never becomes lower than 12.5, which is possibly an overestimation of the real pH. Since Mg is extremely sensitive to pH in the pH range 8.5–12.5 (the extraction test results show that there is a 3 to 4 order of magnitude difference in leached Mg concentration between pH 12.5 and 8.5) and Mg leached concentrations were underestimated by the model (extraction test results) for pH>11, it seems logical that our model underestimates the Mg concentrations in the diffusion test. The previously discussed curves for Pb and Ca, which also have a pH-dependent leaching profile do not show this problem. This can be explained by the much smaller pH-dependency of these elements in the pH range relevant for the diffusion test: there is no or maximum one order of magnitude difference in the Pb and Ca leached concentrations between pH 12.5 and 8.5. The discrepancy for Mg might be overcome by implementing

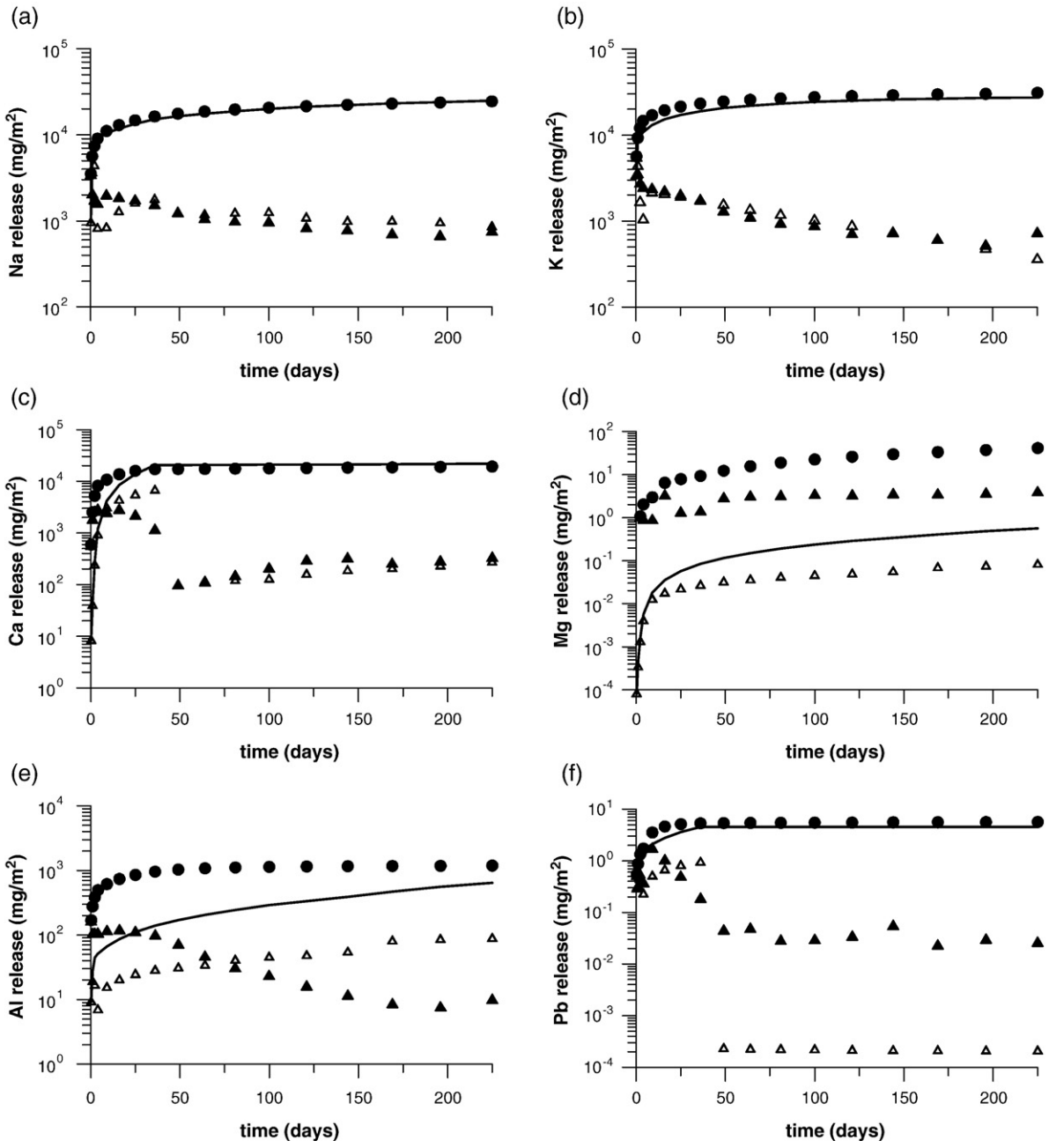


**Fig. 4.** Comparison between calculated (solid line) and measured (full circles) cumulative release of (a) Na, (b) K, (c) Ca, (d) Mg, (e) Al, and (f) Pb for uncarbonated OPC-MSWI bottom ash sample. The non-cumulative amounts are also shown (full triangles for the experimental data and open triangles for the modeled data).

a finer discretisation towards the outer boundary: in this way pH and pore-water concentrations are closer to the real ones and hence dissolution/precipitation reactions are better described. However, this is practically not feasible in the 3D PHREEQC model as calculation times then become extremely long. A better description of the Mg dissolution behaviour may also be obtained by updating the geochemical model in order to adequately describe the leaching profile at high pH (Fig. 1).

The cumulative release of Al is also underpredicted, but the deviation is smaller than for Mg (i.e. less than one order of magnitude at the end of the leaching test). The non-cumulative data points show that for the entire considered timeframe there is a difference of one order of magnitude between measurements and model predictions: an underestimation for the first 75 days and an overestimation afterwards.

## 5. Conclusions

The leaching of major elements and the contaminant Pb from uncarbonated and carbonated cement/waste samples observed in extraction tests and diffusion leach tests was simulated with PHREEQC-2. Overall, the simulated and experimental results are in good agreement. The conceptual model which combined processes of precipitation/dissolution, sorption by surface complexation and formation of solid solutions gave a very good reproduction of the amphoteric Pb leaching. Diffusive transport simulations using the geochemical model derived from the extraction test provided a good description of the diffusion data with the exception of Mg. For the latter element the geochemical model was inappropriate possibly in combination with a too coarse model discretisation towards the outer boundary.

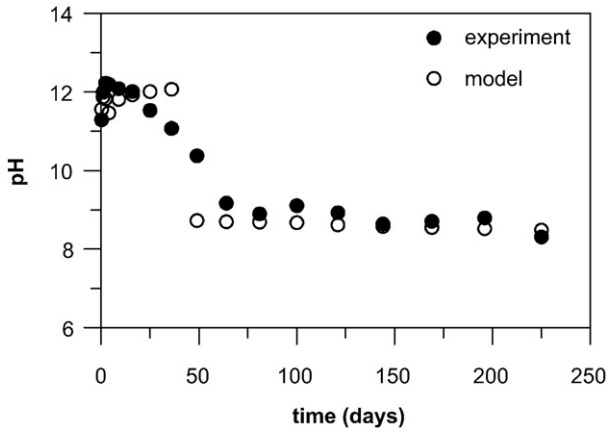


**Fig. 5.** Measured (full circles) and calculated (open circles) pH values of the leachant at the end of each leach period in the diffusion test.

## Appendix A

**Table A1.** Chemical formulas of the minerals present in the CEMDATA07.1 database.

| Mineral name | Chemical formula |
|---|---|
| Portlandite | $Ca(OH)_2$ |
| Jennite-like solid solution end-member | $(CaO)_{1.67}(SiO_2)(H_2O)_{2.1}$ |
| Tobermorite2-like solid solution end-member | $(CaO)_{0.83}(SiO_2)(H_2O)_{1.3}$ |
| Amorphous silica | $SiO_2$ |
| $C_2AH_8$ | $Ca_2Al_2(OH)_{10}\cdot 3H_2O$ |
| $C_2FH_8$ | $Ca_2Fe_2(OH)_{10}\cdot 3H_2O$ |
| Hydrogarnet-OH | $Ca_3Al_2(OH)_{12}$ |
| $C_3FH_6$ | $Ca_3Fe_2(OH)_{12}$ |
| Strätlingite | $Ca_2Al_2SiO_2(OH)_{10}\cdot 3H_2O$ |
| Fe-strätlingite | $Ca_2Fe_2SiO_2(OH)_{10}\cdot 3H_2O$ |
| Hemicarboaluminate | $Ca_4Al_2(CO_3)_{0.5}(OH)_{13}\cdot 5.5H_2O$ |
| Fe-hemicarbonate | $Ca_4Fe_2(CO_3)_{0.5}(OH)_{13}\cdot 5.5H_2O$ |
| Calcite | $CaCO_3$ |
| Ettringite | $Ca_6Al_2(SO_4)_3(OH)_{12}\cdot 26H_2O$ |
| Fe-ettringite | $Ca_6Fe_2(SO_4)_3(OH)_{12}\cdot 26H_2O$ |
| $C_4AH_{13}$ | $Ca_4Al_2(OH)_{14}\cdot 6H_2O$ |
| $C_4FH_{13}$ | $Ca_4Fe_2(OH)_{14}\cdot 6H_2O$ |
| Monosulfoaluminate | $Ca_4Al_2(SO_4)(OH)_{12}\cdot 6H_2O$ |
| Fe-monosulfate | $Ca_4Fe_2(SO_4)(OH)_{12}\cdot 6H_2O$ |
| Monocarboaluminate | $Ca_4Al_2(C0_3)(OH)_{12}\cdot 5H_2O$ |
| Fe-monocarbonate | $Ca_4Fe_2(C0_3)(OH)_{12}\cdot 6H_2O$ |
| Tricarboaluminate | $Ca_6Al_2(CO_3)_3(OH)_{12}\cdot 26H_2O$ |
| Amorphous $Al(OH)_3$ | $Al(OH)_3$ |
| CAH10 | $CaAl_2(OH)_8\cdot 6H_2O$ |
| Siliceous hydrogarnet | $Ca_3Al_2(SiO_4)_{0.8}(OH)_{8.8}$ |
| Anhydrite | $CaSO_4$ |
| Gypsum | $CaSO_4\cdot H_2O$ |
| Hematite | $Fe_2O_3$ |
| $Fe(OH)_{3,mic}$ | $Fe(OH)_3$ |
| Syngenite | $K_2Ca(SO_4)_2\cdot H_2O$ |
| Hydrotalcite | $Mg_4Al_2(OH)_{14}\cdot 3H_2O$ |
| Fe-Hydrotalcite | $Mg_4Fe_2(OH)_{14}\cdot 3H_2O$ |
| $CO_3$-hydrotalcite | $Mg_4Al_2(OH)_{12}CO_3\cdot 3H_2O$ |
| Brucite | $Mg(OH)_2$ |

## References

[1] H.A. van der Sloot, Characterization of the leaching behaviour of concrete mortars and of cement-stabilized wastes with different waste loading for long term environmental assessment, Waste Manag. 22 (2002) 181–186.
[2] J.J. Dijkstra, H.A. van der Sloot, R.N.J. Comans, The leaching of major and trace elements from MSWI bottom ash as a function of pH and time, Appl. Geochem. 21 (2006) 335–351.
[3] J.A. Meima, R.N.J. Comans, Geochemical modeling of weathering reactions in municipal solid waste incinerator bottom ash, Environ. Sci. Technol. 31 (1997) 1269–1276.
[4] J.A. Meima, R.N.J. Comans, The leaching of trace elements from municipal solid waste incinerator bottom ash at different stages of weathering, Appl. Geochem. 14 (1999) 159–171.
[5] A.C. Garrabrants, F. Sanchez, D.S. Kosson, Changes in constituent equilibrium leaching and pore water characteristics of a Portland cement mortar as a result of carbonation, Waste Manag. 24 (2004) 19–36.
[6] T. Astrup, J.J. Dijkstra, R.N.J. Comans, H.A. van der Sloot, T.H. Christensen, Geochemical modeling of leaching from MSWI Air-Pollution-Control Residues, Environ. Sci. Technol. 40 (2006) 3551–3557.
[7] G. Cornelis, T. Van Gerven, C. Vandecasteele, Antimony leaching from uncarbonated and carbonated MSWI bottom ash, J. Hazard. Mater. A137 (2006) 1284–1292.
[8] J.-Y. Park, B. Batchelor, A multi-component numerical leach model coupled with a general chemical speciation code, Water Res. 36 (2002) 156–166.
[9] A.C. Garrabrants, F. Sanchez, D.S. Kosson, Leaching model for a cement mortar exposed to intermittent wetting and drying, AIChE J. 49 (5) (2003) 1317–1333.
[10] L. Tiruta-Barna, A. Imyim, R. Barna, Long-term prediction of the leaching behaviour of pollutants from solidified wastes, Adv. Environ. Res. 8 (2004) 697–711.
[11] L. De Windt, R. Badreddine, Modeling of long-term dynamic leaching tests applied to solidified/stabilised waste, Waste Manag. 27 (11) (2007) 1638–1647.
[12] D.L. Parkhurst, C.A.J. Appelo, User's guide to PHREEQC (version 2)—a computer program for speciation, Batch-Reaction, One-Dimensional Transport and Inverse Geochemical Calculations. Denver, Colorado, USA, Water-Resources Investigations Report 99-4259, 1999.
[13] E. Martens, D. Jacques, T. Van Gerven, L. Wang, D. Mallants, PHREEQC modeling of leaching of major elements and heavy metals from cementitious waste forms, Mater. Res. Soc. Symp. Proc. 1107 (2008) 475–482.
[14] B. Lothenbach, T. Matschei, G. Möschner, F. Glasser, Thermodynamic modeling of the effect of temperature on the hydration and porosity of Portland cement, Cement. Concr. Res. 38 (2008) 1–18.
[15] C. Vandecasteele, G. Wauters, S. Arickx, M. Jaspers, T. Van Gerven, Integrated municipal solid waste treatment using a grate furnace incinerator: the Indaver case, Waste Manag. 27 (10) (2007) 1366–1375.
[16] D.S. Kosson, H.A. van der Sloot, F. Sanchez, A.C. Garrabrants, An integrated framework for evaluating leaching in waste management and utilization of secondary materials, Environ. Eng. Sci. 19 (3) (2002) 159–204.
[17] T. Van Gerven, G. Cornelis, E. Vandoren, A.C. Garrabrants, F. Sanchez, D.S. Kosson, C. Vandecasteele, Effects of progressive carbonation on heavy metal leaching from waste-containing cement matrices, AIChE J. 52 (2006) 826–837.
[18] Nederlands Normalisatie Instituut (NNI), NEN 7345, Uitloogkarakteristieken van vaste grond-en steenachtige bouwmaterialen en afvalstoffen–Uitloogproeven–Bepaling van de uitloging van anorganische componenten uit vormgegeven en monolithische materialen met de diffusieproef, Delft, The Netherlands, 1995.
[19] T.G. Ferdelman, The distribution of sulfur, iron, manganese, copper and uranium in salt marsh sediment cores as determined by sequential extraction methods, Master thesis, University of Delaware, 1988.
[20] M.L. Jackson, C.H. Lim, L.W. Zelazny, Oxides, hydroxides, and aluminosilicates, in: A. Klute (Ed.), Methods of Soil Analysis Part I—Physical and Mineralogical Methods, SSSA, Madison, Wisconsin, 1996, pp. 113–118.
[21] E. Martens, Modeling Leaching of Inorganic Contaminants from Cementitious Waste Matrices, Master thesis, University of Leuven, Leuven, 2007.
[22] D.A. Kulik, GEMS-PSI 2.2, PSI-Villigen, Switzerland, 2007 available at http://gems.web.psi.ch/.
[23] D. Jacques, Benchmarking of the cement model and detrimental chemical reactions including temperature dependent parameters, NIRAS/ONDRAF technical report NIROND-TR 2008-30E, 2008.
[24] C.S. Kirby, J.D. Rimstidt, Interaction of municipal solid waste ash with water, Environ. Sci. Technol. 28 (1994) 443–451.
[25] A. Godelitsas, J.M. Astilleros, K. Hallam, S. Harissopoulos, A. Putnis, Interaction of calcium carbonates with lead in aqueous solutions, Environ. Sci.Technol. 37 (2003) 3351–3360.
[26] A.A. Rouff, E.J. Elzinga, R.J. Reeder, N.S. Fisher, The influence of pH on the kinetics, reversibility and mechanisms of Pb(II) sorption at the calcite–water interface, Geochim. Cosmochim. Acta 69 (2005) 5173–5186.
[27] B. Lothenbach, M. Ochs, H. Wanner, M. Yui, Thermodynamic data for the speciation and solubility of Pd, Pb, Sn, Sb, Nb and Bi in aqueous solution, Japan Nuclear Cycle Development Institute (JNC), Report TN8400 99-011, 1999.
[28] D.A. Dzombak, F.M.M. Morel, Surface Complexation Modeling—Hydrous Ferric Oxide, John Wiley & Sons, Inc., New York, 1990.
[29] J.A. Meima, R.N.J. Comans, Application of surface complexation/precipitation modeling to contaminant leaching from weathered municipal solid waste incinerator bottom ash, Environ. Sci. Technol. 32 (1998) 688–693.
[30] C. Jing, X. Meng, G.P. Korfiatis, Lead leachability in stabilized/solidified soil samples evaluated with different leaching tests, J. Hazard. Mater. B114 (2004) 101–110.
[31] C.E. Halim, S.A. Short, J.A. Scott, R. Amal, G. Low, Modeling the leaching of Pb, Cd, As, and Cr from cementitious waste using PHREEQC, J. Hazard. Mater. A125 (2005) 45–61.
[32] Y. Xu, T. Boonfueng, L. Axe, S. Maeng, T. Tyson, Surface complexation of Pb(II) on amorphous iron oxide and manganese oxide: spectroscopic and time studies, J. Colloid Interface Sci. 299 (2006) 28–40.
[33] M. Fan, T. Boonfueng, Y. Xu, L. Axe, T.A. Tyson, Modeling Pb sorption to microporous amorphous oxides as discrete particles and coatings, J. Colloid Interface Sci. 281 (2005) 39–48.
[34] M.L.D. Cougar, B.E. Scheetz, D.M. Roy, Ettringite and C–S–H Portland cement phases for waste ion immobilization: a review, Waste Manag. 16 (1996) 295–303.
[35] C.A. Johnson, M. Kersten, Solubility of Zn(II) in association with calcium silicate hydrates in alkaline solutions, Environ. Sci. Technol. 33 (1999) 2296–2298.
[36] I. Moulin, W.E.E. Stone, J. Sanz, J.-Y. Bottero, F. Mosnier, C. Haehnel, Lead and Zinc retention during hydration of tri-calcium silicate: a study by sorption isotherms

and 29Si nuclear magnetic resonance spectroscopy, Langmuir 15 (1999) 2829–2835.
[37] J. Rose, I. Moulin, J. Hazemann, A. Masion, P.M. Bertsch, J. Bottero, F. Mosnier, C. Haehnel, X-ray absorption spectroscopy study of immobilization processes for heavy metals in calcium silicate hydrates: 1. Case of lead, Langmuir 16 (2000) 9900–9906.
[38] C.A. Johnson, Metal Binding in the Cement Matrix. An Overview of our Current Knowledge, Dept. Water Resources and Drinking Water, Water–rock Interaction Group, EAWAG, Duebendorf, Switzerland, 2002.
[39] R. Badreddine, A.-N. Humez, U. Mingelgrin, A. Benchara, F. Meducin, R. Prost, Retention of trace metals by solidified/stabilized wastes: assessment of long-term metal release, Environ. Sci. Technol. 38 (2004) 1383–1398.
[40] C.E. Halim, R. Amal, D. Beydoun, J.A. Scott, G. Low, Implications of the structure of cementitious wastes containing Pb(II), Cd(II), As(V), and Cr(VI) on the leaching of metals, Cem. Concr. Res. 34 (2004) 1093–1102.
[41] V. Mijno, L.J.J. Catalan, F. Martin, J.-C. Bollinger, Compositional changes in cement-stabilized waste during leach tests—comparison of SEM/EDX data with predictions from geochemical speciation modeling, J. Colloid Interface Sci. 280 (2004) 465–477.
[42] L. Vinckx, Gebruik van mobiele componenten bij de uitloging van zware metalen uit secundaire grondstoffen. Thesis, Katholieke Hogeschool Leuven, Leuven, Belgium, 2003.
[43] T. Van Gerven, Leaching of heavy metals from carbonated waste-containing construction material. PhD Thesis, Katholieke Universiteit Leuven, Leuven, Belgium, 2005.
[44] L. Wang, Near-field chemistry of a HLW/SF repository in Boom Clay—scoping calculations relevant to the supercontainer design, External report of the Belgian Nuclear Research Centre. Mol, Belgium, SCK-CEN-ER-17, 2006.
[45] H.J.H. Brouwers, R.J. van Eijk, Alkali concentrations of pore solution in hydrating OPC, Cem. Concr. Res. 33 (2003) 191–196.
[46] J.A. Meima, R.N.J. Comans, Reducing Sb-leaching from municipal solid waste incinerator bottom ash by addition of sorbent minerals, J. Geochem. Explor. 62 (1998) 299–304.
[47] H.A. van der Sloot, A. van Zomeren, J.J. Dijkstra, J.C.L. Meeussen, R.N.J. Comans, H. Scharff, Prediction of the Leaching Behaviour of Waste Mixtures by Chemical Speciation Modeling Based on a Limited Set of Key Parameters, 2005 ECN-RX–05-164.
[48] L. Tiruta-Barna, Z. Rethy, R. Barna, Release dynamic process identification for a cement based material in various leaching conditions. Part II. Modeling the release dynamics for different leaching conditions, J. Environ. Manag. 74 (2005) 127–139.
[49] W.J. MacCarter, G. Starrs, T.M. Chrisp, Electrical conductivity, diffusion, and permeability of Portland cement-based mortars, Cem. Concr. Res. 30 (2000) 1395–1400.
[50] A. Van Geen, A.P. Robertson, J.O. Leckie, Complexation of carbonate species at the goethite surface—implications for adsorption of metal ions in natural-waters, Geochim. Cosmochim. Acta 58 (9) (1994) 2073–2086.